Full Paper

Synthesis of Pyrimidones and Evaluation of Their Xanthine Oxidase Inhibitory and Antioxidant Activities

Handuvinahalli Devanna Gurupadaswamy[1], Virupaksha Girish[1], Farhan Zameer[2], Raghavendra Hegdekatte[2], Jyoti Bala Chauhan[2], and Shaukath Ara Khanum[1]

[1] Department of Chemistry, Yuvaraja's College Mysore, University of Mysore, Mysore, Karnataka, India
[2] Mahajana Life Science Research Laboratory, Department of Biotechnology, Microbiology and Biochemistry, Mahajana Research Foundation, Pooja Bhagavat Memorial Mahajana Post Graduate Centre, Affiliated to University of Mysore, Metagalli, Mysore, Karnataka, India

The increasing prevalence of gout has been accompanied by a growing number of patients intolerant to or with disease refractory to the available urate-lowering therapies. This metabolic disease is a common disease with a higher prevalence in men older than 30 years and in women older than 50 years. These findings highlight the need for emerging treatments to effectively lower urate levels. In this view, we describe the xanthine oxidase (XO) inhibitory activities of the synthesized compounds **5a–j** and also their antioxidant activities. Compounds **5c**, **5d**, **5f**, **5h**, and **5j** exhibited good inhibitory activities against XO. On the other hand, compounds **5g** and **5j** exhibited moderate antioxidant activity.

Keywords: Antioxidant activity / Pyrimidones / Xanthine oxidase inhibitory activity

Received: June 24, 2013; Revised: August 13, 2013; Accepted: August 15, 2013

DOI 10.1002/ardp.201300240

Introduction

Enzyme inhibitors are molecules that bind to enzymes and decrease their activity [1]. Since blocking an enzyme's activity can kill a pathogen or correct a metabolic imbalance, many drugs are enzyme inhibitors [2]. The design of the inhibitors, based on the structure of an enzyme active site, is helpful to determine the 3D structure of the enzyme and of the enzyme in complex with an inhibitor at high resolution. Precisely all the molecule interactions that are necessary for a drug to bind to its target site based on the architecture of enzymes active site and the interactions that stabilize the inhibitor with greater binding affinity can be designed with a shape that fits better into the active site and with charge distributed suitable for increased interaction energies. Also, it may involve topographic studies [3, 4]. The enzyme xanthine oxidase (XO), also known as xanthine oxidoreductase (XOR), helps in the breakdown of purine to uric acid [5] and overproduction of uric acid leads to hyperuricemia, which is linked to gout [6]. Gout is characterized by the deposition of uric acid in the joints leading to severe and episodic painful inflammation [7]. Recent epidemiological studies revealed that the overall disease burden of gout worldwide is increasing [8]. XOR is a complex molybdoflavor enzyme present in two different functional forms: dehydrogenase and XO [9]. XO is a critical source of reactive oxygen species (ROS) that contribute to vascular inflammation [10]. Under normal physiological conditions, it is mainly found in the dehydrogenase form, while in inflammatory situations, post-translational modification converts the dehydrogenase form into XO. These inflammatory conditions lead to an increase in XO levels and thus an increased ROS generation by the enzymatic process, finally resulting in alterations in vascular function [9]. It has also been shown that XO secondarily leads to peroxy nitrite formation. Peroxy nitrite is one of the most powerful ROS that is produced by the reaction of nitric oxide and superoxide radicals, and is considered to be a marker for reactive nitrogen species, accompanied by oxidative stress [11, 12]. Both XO and dehydrogenase form catalyze the removal of hydrogen from a substrate using oxygen as hydrogen acceptor, and it gets reduced. During reoxygenation (i.e., reperfusion phase) it reacts with molecular oxygen, thereby releasing superoxide anion radicals. The XO pathway has been implicated as an important route in the oxidative injury to tissue, especially after ischemia–reperfusion [13].

Correspondence: Dr. Shaukath Ara Khanum, Department of Chemistry, Yuvaraja's College, University of Mysore, Mysore 570 006, India.
E-mail: shaukathara@yahoo.co.in
Fax: +91 821 2419239

Nitrogen heterocycles in general and pyrimidine and its analogs in particular are the most explored fields in heterocyclic chemistry due to their diverse biological activities [14–16]. Pyrimidine, being an integral part of DNA and RNA, plays a vital role in several biological processes, and diverse biological properties have been associated with numerous fused pyrimidines including XO inhibition [17], anti-inflammatory [18], anti-allergic [19], hypnotic [20], antiviral [21], anti-microbial [22], and antioxidant activity [23]. The above-mentioned biological importance of pyrimidones led us to synthesize novel pyrimidine analogs comprising hydrazide linkage. In continuation of our studies in the area of XO inhibitors [24] and with a view to the synthesis of novel pyrimidones, we herein report design, synthesis, and XO inhibition and antioxidant activity of pyrimidones.

Results and discussion

The inhibition activity of synthesized compounds **5a–j** was tested against XO [25, 26]. The rate of formation of uric acid from oxidation of xanthine in the presence of **5a–j** inhibitors against rat liver XO was studied. The inhibitory activity of the compounds **5a–j** against XO was compared with standard drug allopurinol (Table 1). The known X-ray structure of xanthine oxidoreductase bound molecule shows highly specific binding pocket presenting a long narrow cavity leading toward the Mo(IV) complex. Molybdenum protein sites of both XO and xanthine dehydrogenase are structurally equivalent. Further, to understand the binding mode of newly synthesized compounds **5a–j** with XO, molecular docking studies of the most potent compounds (**5c**, **5d**, and **5f**) and the structure of XO (PDB entry code: 2CKJ) was obtained and analyzed [27]. It is possible that phenyl moiety binds to active site and heterocyclic ring may bind to the peripheral site of enzyme and transfer electrons to molybdenum center (a2) electron acceptor from no site of XO. Different heterocyclic amides **5a–j** were tested for their ability to block the XO activity for the substrate xanthine. The order of *in vitro* inhibitory activity of the title compounds against rat liver XO is found to be **5c** > **5d** > **5f** > **5h** > **5j**; however other compounds in the series were very poor XO inhibitors and the activity was not in a detectable range. The present study helps to understand structure-activity relationship mode of interaction and extent of inhibition of compounds **5a–j** against rat liver (*in vitro*) and human milk (*in silico*) of XO.

A series of assays were then performed in order to evaluate the antioxidant properties of the synthesized compounds **5a–j**. The 1,1-diphenyl-2-picrylhydrazyl (DPPH) radical scavenging assay is widely used to investigate the radical scavenging activities of several natural as well as synthetic compounds [28]. The scavenging activity has been studied in the process of hydrogen atom transfer to the stable free radical DPPH to compare the activity of compounds under investigation with that of widely known antioxidant parameter. Free radical scavenging activity of DPPH is a stable free radical at room temperature and accepts an electron or hydrogen radical to become a stable diamagnetic molecule. The reduction capability of DPPH radicals was determined by decreased absorbance at 517 nm, which is induced by antioxidants. The recent study was carried out to determine the hydrogen-donating capabilities of the compounds **5a–j**. The results are summarized in Fig. 1. Compound **5g** with trifluoro methyl group and compound **5j** with *N*,*N*-dimethyl amino group showed moderate activity compared with the standard synthetic antioxidant butylated hydroxyl anisole (BHA) whereas the other compounds displayed mild activity. The IC_{50} value of the standard BHA in DPPH method was found to be 13.81 μg/mL, whereas the IC_{50} values of the compounds **5g** and **5j** were found to be 35.81 and 17.45 μg/mL, respectively (Fig. 1).

Lipid peroxidation (LPO) refers to the oxidative degradation of lipids. It is the process in which free radicals steal electrons from the lipids in cell membranes, resulting in cell damage.

Table 1. Comparative inhibitory activities of compounds **5a–j** (15 μM) against rat liver xanthine oxidase in percentage inhibition.

Compounds	Rat liver
5a	ND
5b	ND
5c	55%
5d	45%
5e	ND
5f	40%
5g	ND
5h	32%
5i	ND
5j	15%
Allopurinol	100%

ND, not detected.

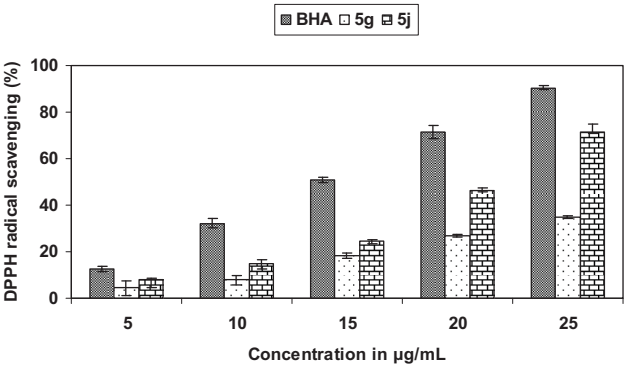

Figure 1. DPPH scavenging assay of potent compounds **5g** and **5j**.

The LPO activities of compounds **5g**, **5j**, and BHA had the IC_{50} values of 33.69, 18.13, and 13.72 μg/mL, respectively (Fig. 2).

To substantiate the result of DPPH radical scavenging activity the reducing power of the compounds **5a–j** was also evaluated. Reducing power assay was determined based on the principle that substances that have reduction potential react with potassium ferricyanide to form potassium ferocyanide, which then reacts with ferric chloride to form ferric–ferrous complex that has maximum absorption at 700 nm. At the concentration of 25 μg/mL compound **5g** showed threefold and compound **5j** showed twofold lesser reducing power ability than the standard (Fig. 3).

The damaging action of hydroxyl radicals is the strongest among free radicals. In biochemical systems, superoxide radical is converted by superoxide dismutase to hydrogen peroxide, which can subsequently generate extremely reactive hydroxyl radicals in the presence of certain transition metal ions. Further, hydroxyl radical has the capacity to cause DNA strand breakage and leads to mutations. Compounds **5g**, **5j**, and BHA displayed hydroxyl radical scavenging activity with IC_{50} values of 39.88, 23.85, and 14.49 μg/mL, respectively (Fig. 4).

Chelation of transition metals prevents catalysis of hydrogen peroxide decomposition and Fenton type reaction. In presence of chelating agents, the complex formation is disrupted with the result that the red color of the complex is decreased. The transition metal ion Fe^{2+} possesses the ability to move single electrons by virtue of which it can allow the formation and propagation of many radical reactions. Metal chelating ability was also accessed for the compounds **5g**, **5j**, and EDTA with IC_{50} values of 31.25, 17.56, and 13.97 μg/mL, respectively (Fig. 5).

The mode of interaction was analyzed by docking using human milk XO (PDB entry code: 2CKJ) on selected active site of amino acids of chain C and molybdenum. Among the title compounds the best three entities, namely, **5c**, **5d**, and **5f**, were subjected for structure–activity relationship and their structure permitted various modes of interaction with active site of amino acid. Compound **5c** produced relatively better activity against human milk XO with atomic contact energy of −156.41 followed by **5d** (−131.51), **5f** (−127.55) than compared to standard drug allopurinol (−280.71), respectively.

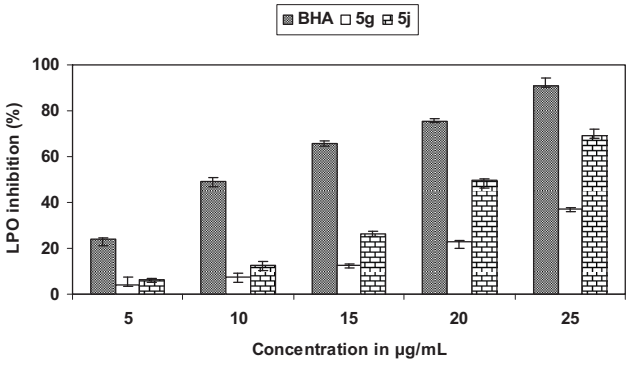

Figure 2. Inhibition of lipid peroxidation by potent compounds **5g** and **5j**.

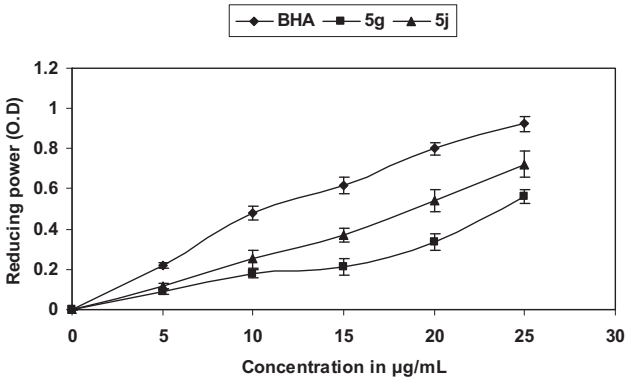

Figure 3. Reducing power assay of potent compounds **5g** and **5j**.

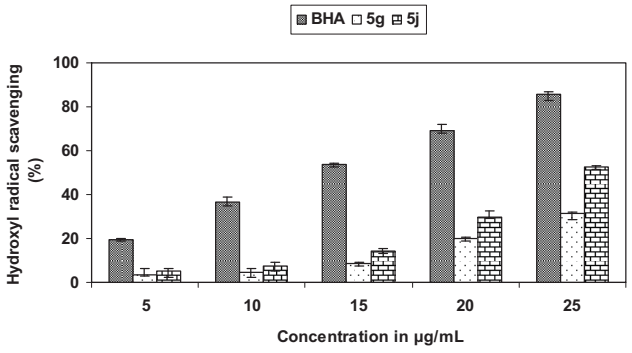

Figure 4. Hydroxyl radical scavenging assay of potent compounds **5g** and **5j**.

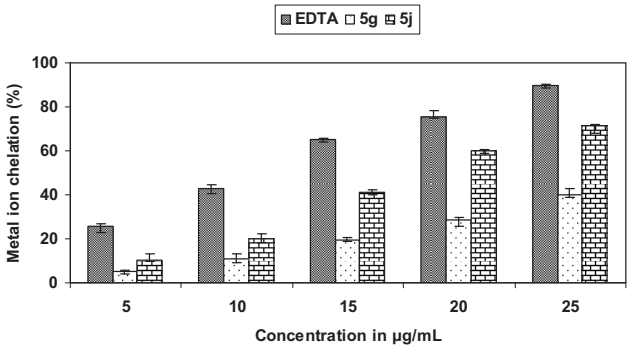

Figure 5. Metal ion chelation assay of potent compounds **5g** an **5j**.

Conclusion

From the results of the present study, it is concluded that a series of novel pyrimidones were synthesized and their XO inhibitory activities were evaluated. Compounds **5c**, **5d**, **5f**, **5h**, and **5j** exhibited good inhibitory activities against XO. On the other hand, compounds **5g** and **5j** exhibited good antioxidant activity.

Experimental

Chemistry

Materials and methods

Chemicals were purchased from Sigma–Aldrich Chemical Co. TLC was performed on aluminum-baked silica plates and visualized by UV light. Melting points were determined on a Thomas Hoover capillary melting point apparatus with a digital thermometer. IR spectra were recorded on a FT-IR Shimadzu 8300 spectrophotometer, ^{1}H NMR spectra were recorded on a Bruker 400 MHz NMR spectrophotometer in DMSO-d_6, and chemical shift were recorded in parts per million downfield from tetramethyl silane. Mass spectra were obtained with a VG70-70H spectrophotometer, and important fragments are given with the relative intensities in brackets. Elemental analysis results are within 0.4% of the calculated value.

*Synthesis and characterization of compounds **3a–3j***

Synthesis of 4-chlorobenzoic acid-*N*-(2-chloro acetyl) hydrazide (**3a**) (Scheme 1): Chloroacetic acid (**2**, 1.46 g, 12.9 mmol) was dissolved in dichloromethane (20 mL), 2,6-lutidine (4.14 mL, 38.7 mmol), TBTU (4.24 g, 12.9 mmol) was added, and the reaction mixture was stirred for 10 min at 25°C. To the reaction mixture 4-chlorobenzoic acid hydrazide (**1a**, 2.0 g, 11.7 mmol) was added dropwise and it was stirred at ambient temperature for 3 h. After completion of the reaction, monitored by TLC, the reaction mass was quenched with 10% sodium bicarbonate solution (20 mL). The solid precipitated was filtered, washed with water (3 × 20 mL), and dried to obtain compound **3a** as white solid.

Yield: 88%; mp: 188–190°C; IR (KBr): 1645 (amide, C=O); 3760–3525 cm^{-1} (NH–NH); ^{1}H NMR (DMSO-d_6) δ: 4.51 (s, 2H, CH_2), 7.50–7.54 (d, 2H, Ar-H); 7.81–7.84 (d, 2H, Ar-H); 9.85 (bs, 1H, NH); 10.05 (bs, 1H, NH); MS (EI): *m/z* (75%) M$^+$ 247; Anal. calcd. for $C_9H_8Cl_2N_2O_2$ (247): C, 43.75; H, 3.26; Cl, 28.70; N, 11.34. Found: C, 43.88; H, 3.19; Cl, 28.64; N, 11.33%.

3b: Yield: 81%; mp: 189.8–190.5°C; IR (KBr): 1630 (amide, C=O); 3720–3515 cm^{-1} (NH–NH); ^{1}H NMR (DMSO-d_6) δ: 4.20 (s, 2H, CH_2), 7.71–7.74 (d, 2H, Ar-H); 7.80–7.82 (d, 2H, Ar-H); 10.40 (bs, 1H, NH); 10.63 (bs, 1H, NH); MS (EI): *m/z* (75%) M$^+$ 291; Anal. calcd. for $C_9H_8BrClN_2O_2$ (291): C, 37.08; H, 2.77; Br, 27.41; Cl, 12.16; N, 9.61. Found: C, 37.15; H, 2.82; Cl, 12.14; N, 9.57%.

3c: Yield: 81%; mp: 221–222°C; IR (KBr): 1650 (amide, C=O); 3750–3555 cm^{-1} (NH–NH); ^{1}H NMR (DMSO-d_6) δ: 4.20 (s, 2H, CH_2), 7.64–7.66 (d, 2H, Ar-H); 7.88–7.91 (d, 2H, Ar-H); 10.1 (bs, 2H, NH); 10.55 (bs, 2H, NH); MS (EI): *m/z* (74%) M$^+$ 338; Anal. calcd. for $C_9H_8ClIN_2O_2$ (338): C, 31.93; H, 2.38; Cl, 10.47; I, 37.49; N, 8.28; O, 9.45. Found: C, 31.85; H, 2.29; Cl, 10.58; N, 8.36%.

3d: Yield: 80%; mp: 178–180°C; IR (KBr): 1640 (amide, C=O); 3690–3535 cm^{-1} (NH–NH); ^{1}H NMR (DMSO-d_6) δ: 2.36 (s, 3H, CH_3), δ: 4.19 (s, 2H, CH_2), 7.29–7.31 (d, 2H, Ar-H); 7.76–7.79 (d, 2H, Ar-H); 10.2 (bs, 1H, NH); 10.43 (bs, 1H, NH); MS (EI): *m/z* (72%) M$^+$ 226; Anal. calcd. for $C_{10}H_{11}ClN_2O_2$ (226): C, 52.99; H, 4.89; Cl, 15.64; N, 12.36. Found: C, 52.81; H, 4.75; Cl, 15.80; N, 12.25%.

3e: Yield: 73%; mp: 114–118°C; IR (KBr): 1615 (amide, C=O); 3720–3515 cm^{-1} (NH–NH); ^{1}H NMR (DMSO-d_6) δ: 1.31 (s, 9H, $(CH_3)_3$), 4.27 (s, 2H, CH_2), 7.80–7.82 (d, 2H, Ar-H); 7.92–7.94 (d, 2H, Ar-H); 10.3 (bs, 1H, NH); 10.62 (bs, 1H, NH); MS (EI): *m/z* (74%) M$^+$ 268; Anal. calcd. for $C_{13}H_{17}ClN_2O_2$ (268): C, 58.10; H, 6.38; Cl, 13.19; N, 10.42. Found: C, 58.22; H, 6.45; Cl, 13.30; N, 10.49%.

3f: Yield: 77%; mp: 198–199°C; IR (KBr): 1635 (amide, C=O); 3685–3545 cm^{-1} (NH–NH); ^{1}H NMR (DMSO-d_6) δ: 3.83 (s, 3H, CH_3), δ: 4.20 (s, 2H, CH_2), 7.03–7.05 (d, 2H, Ar-H); 7.85–7.88 (d, 2H, Ar-H); 10.31 (bs, 1H, NH); 10.38 (bs, 1H, NH); MS (EI): *m/z* (74%) M$^+$ 242; Anal. calcd. for $C_{10}H_{11}ClN_2O_3$ (242): C, 49.50; H, 4.57; Cl, 14.61; N, 11.54. Found: C, 49.55; H, 4.62; Cl, 14.75; N, 11.65%.

3g: Yield: 74%; mp: 205–208°C; IR (KBr): 1630 (amide, C=O); 3740–3515 cm^{-1} (NH–NH); ^{1}H NMR (DMSO-d_6) δ: 4.22 (s, 2H, CH_2), 7.89–7.91 (d, 2H, Ar-H); 8.05–8.07 (d, 2H, Ar-H); 10.48 (bs, 1H, NH); 10.79 (bs, 1H, NH); MS (EI): *m/z* (74%) M$^+$ 280; Anal. calcd. for $C_{10}H_8ClF_3N_2O_2$ (280) C, 42.80; H, 2.87; Cl, 12.63; F, 20.31; N, 9.98. Found: C, 42.80; H, 2.92; Cl, 12.68; F, 20.38; N, 10.05%.

3h: Yield: 81%; mp: 189–192°C; IR (KBr): 1640 (amide, C=O); 3720–3545 cm^{-1} (NH–NH); ^{1}H NMR (DMSO-d_6) δ: 4.19 (s, 2H, CH_2), 7.48–7.51 (d, 2H, Ar-H); 7.97–8.00 (d, 2H, Ar-H); 10.5 (bs, 2H, NH); 10.79 (bs, 1H, NH); MS (EI): *m/z* (75%) M$^+$ 296; Anal. calcd. for $C_{10}H_8ClF_3N_2O_3$ (296): C, 40.49; H, 2.72; Cl, 11.95; F, 19.21; N, 9.44. Found: C, 40.58; H, 2.81; Cl, 12.05; F, 19.25; N, 9.55%.

3i: Yield: 82%; mp: 226–228°C; IR (KBr): 1650 (amide, C=O); 3670–3555 cm^{-1} (NH–NH); ^{1}H NMR (DMSO-d_6) δ: 4.23 (s, 2H, CH_2), 8.09–8.12 (d, 2H, Ar-H); 8.35–8.37 (d, 2H, Ar-H); 10.45 (bs, 1H, NH); 10.85 (bs, 1H, NH); MS (EI): *m/z* (74%) M$^+$ 257; Anal. calcd. for $C_9H_8ClN_3O_4$ (257): C, 41.96; H, 3.13; Cl, 13.76; N, 16.31. Found: C, 42.06; H, 3.24; Cl, 13.85; N, 16.42%.

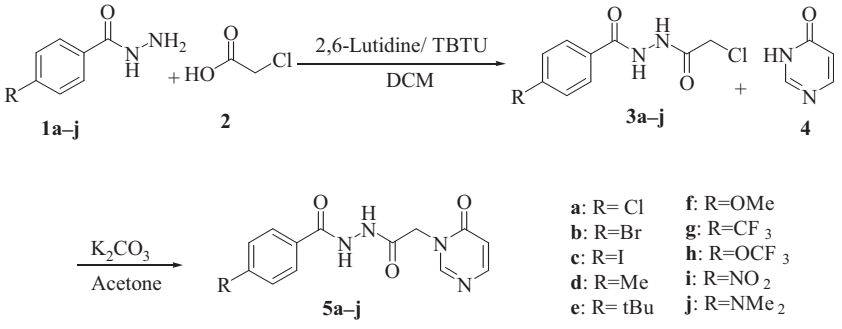

Scheme 1. Synthesis of pyrimidone derivatives.

3j: Yield: 80%; mp: 188–191°C; IR (KBr): 1655 (amide, C=O); 3750–3535 cm^{-1} (NH–NH); ^1H NMR (DMSO-d_6) δ: 2.97 (s, 6H, $2CH_3$), 4.18 (s, 2H, CH_2), 6.69–6.72 (d, 2H, Ar-H); 7.72–7.75 (d, 2H, Ar-H); 10.14 (bs, 2H, NH); 10.5 (bs, 2H, NH); MS (EI): *m/z* (74%) M^+ 255; Anal. calcd. for $C_{11}H_{14}ClN_3O_2$ (255): C, 51.67; H, 5.52; Cl, 13.87; N, 16.43. Found: C, 51.80; H, 5.60; Cl, 13.95; N, 16.51%.

*Synthesis and characterization of compounds **5a–5j***

Synthesis of 4-chloro benzoic acid-*N*-[2-(6-oxo-6H-pyrimidin-1-yl)-acetyl]-hydrazide (**5a**) (Scheme 1): To a solution of compound (**3a**, 1.0 g, 4.0 mmol) and 3H-pyrimidin-4-one (**4**, 0.39 g, 4.0 mmol) in acetone (20 mL), potassium carbonate (1.68 g, 12.1 mmol) was added and the reaction mixture was heated to 55°C for 12 h under inert atmosphere. After the completion of reaction monitored by TLC, the reaction mixture was cooled to 25°C, filtered to remove potassium carbonate, and washed with acetone (3×20 mL), and the mother liquor was concentrated. The crude product was purified by column chromatography using silica gel as stationary phase and hexane/ethyl acetate as mobile phase to achieve compound **5a** as white solid.

Yield: 47%; mp: 245–247°C; IR (KBr): 1610 (C=O); 1655 (amide, C=O); 3710–3505 cm^{-1} (NH–NH); ^1H NMR (DMSO-d_6) δ: 4.74 (s, 2H, CH_2); 6.1–6.24 (d, 1H, pyrimidone-H at sixth position); 6.57–6.64 (d, 1H, pyrimidone-H at fifth position); 7.35–7.42 (d, 2H, Ar-H); 7.5–7.55 (s, 1H, pyrimidone-H at second position); 7.8–7.85 (d, 2H, Ar-H); 10.71 (bs, 2H, NH); MS (EI): *m/z* (75%) M^+ 306; Anal. calcd. for $C_{13}H_{11}ClN_4O_3$ (306): C, 50.91; H, 3.61; Cl, 11.56; N, 18.27. Found: C, 51.02; H, 3.58; Cl, 11.48; N, 18.36%.

5b: Yield: 41%; mp: 270–272°C; IR (KBr): 1615 (C=O); 1615 (amide, C=O); 3690–3525 cm^{-1} (NH–NH); ^1H NMR (DMSO-d_6) δ: 4.7 (s, 2H, CH_2); 6.2–6.25 (d, 1H, pyrimidone-H at sixth position); 6.56–6.66 (d, 1H, pyrimidone-H at fifth position); 7.33–7.45 (d, 2H, Ar-H); 7.5–7.6 (s, 1H, pyrimidone-H at second position); 7.79–7.83 (d, 2H, Ar-H); 10.75 (bs, 2H, NH); MS (EI): *m/z* (74%) M^+ 351; Anal. calcd. for $C_{13}H_{11}BrN_4O_3$ (351): C, 44.46; H, 3.16; Br, 22.75; N, 15.95. Found: C, 44.59; H, 3.28; Br, 22.64; N, 15.85%.

5c: Yield: 48%; mp: 282–284°C; IR (KBr): 1620 (C=O); 1625 (amide, C=O); 3705–3535 cm^{-1} (NH–NH);^1H NMR (DMSO-d_6) δ: 4.65 (s, 2H, CH_2); 6.2–6.25 (d, 1H, pyrimidone-H at sixth position); 6.55–6.7 (d, 1H, pyrimidone-H at fifth position); 7.3–7.45 (d, 2H, Ar-H); 7.55–7.6 (s, 1H, pyrimidone-H at second position); 7.78–7.82 (d, 2H, Ar-H); 10.65 (bs, 2H, NH); MS (EI): *m/z* (74%) M^+ 398; Anal. calcd. for $C_{13}H_{11}IN_4O_3$ (398): C, 39.22; H, 2.78; I, 31.87; N, 14.07. Found: C, 39.29; H, 2.91; I, 31.97; N, 14.15%.

5d: Yield: 55%; mp: 239–241°C; IR (KBr): 1610 (C=O); 1635 (amide, C=O); 3725–3540 cm^{-1} (NH–NH); ^1H NMR (DMSO-d_6) δ: 2.38 (s, 3H, CH_3); 4.65 (s, 2H, CH_2); 6.2–6.25 (d, 1H, pyrimidone-H at sixth position); 6.55–6.64 (d, 1H, pyrimidone-H at fifth position); 7.35–7.4 (d, 2H, Ar-H); 7.5–7.6 (s, 1H, pyrimidone-H at second position); 7.75–7.82 (d, 2H, Ar-H); 10.74 (bs, 2H, NH); MS (EI): *m/z* (73%) M^+ 286; Anal. calcd. for $C_{14}H_{14}N_4O_3$ (286): C, 58.73; H, 4.93; N, 19.57. Found: C, 58.65; H, 5.05; N, 19.68%.

5e: Yield: 46%; mp: 214–216°C; IR (KBr): 1615 (C=O); 1645 (amide, C=O); 3700–3505 cm^{-1} (NH–NH); ^1H NMR (DMSO-d_6) δ: 1.29 (s, 9H, tBu); 4.6 (s, 2H, CH_2); 6.2–6.26 (d, 1H, pyrimidone-H at sixth position); 6.52–6.6 (d, 1H, pyrimidone-H at fifth position); 7.3–7.45 (d, 2H, Ar-H); 7.54–7.6 (s, 1H, pyrimidone-H at second position); 7.75–7.82 (d, 2H, Ar-H); 10.65 (bs, 2H, NH); MS (EI): *m/z* (75%) M^+ 328; Anal. calcd. for $C_{17}H_{20}N_4O_3$ (328): C, 62.18; H, 6.14; N, 17.06. Found: C, 62.06; H, 6.31; N, 17.18%.

5f: Yield: 61%; mp: 253–253°C; IR (KBr): 1610 (C=O); 1625 (amide, C=O); 3720–3510 cm^{-1} (NH–NH); ^1H NMR (DMSO-d_6) δ: 3.82 (s, 3H, OCH_3); 4.73 (s, 2H, CH_2); 6.1–6.3 (d, 1H, pyrimidone-H at sixth position); 6.5–6.6 (d, 1H, pyrimidone-H at fifth position); 7.23–7.4 (d, 2H, Ar-H); 7.5–7.6 (s, 1H, pyrimidone-H at second position); 7.72–7.83 (d, 2H, Ar-H); 10.7 (bs, 2H, NH); MS (EI): *m/z* (72%) M^+ 303; Anal. calcd. for $C_{14}H_{14}N_4O_4$ (302): C, 55.63; H, 4.67; N, 18.53. Found: C, 55.72; H, 4.78; N, 18.45%.

5g: Yield: 65%; mp: 265–267°C; IR (KBr): 1610 (C=O); 1665 (amide, C=O); 3695–3515 cm^{-1} (NH–NH); ^1H NMR (DMSO-d_6) δ: 4.75 (s, 2H, CH_2); 6.2–6.32 (d, 1H, pyrimidone-H at sixth position); 6.54–6.65 (d, 1H, pyrimidone-H at fifth position); 7.2–7.4 (d, 2H, Ar-H); 7.55–7.63 (s, 1H, pyrimidone-H at second position); 7.75–7.85 (d, 2H, Ar-H); 10.75 (bs, 2H, NH); MS (EI): *m/z* (74%) M^+ 340; Anal. calcd. for $C_{14}H_{11}F_3N_4O_3$ (340): C, 49.42; H, 3.26; F, 16.75; N, 16.47. Found C, 49.55; H, 3.33; F, 16.64; N, 16.38%.

5h: Yield: 63%; mp: 233–235°C; IR (KBr): 1620 (C=O); 1675 (amide, C=O); 3720–3510 cm^{-1} (NH–NH); ^1H NMR (DMSO-d_6) δ: 4.73 (s, 2H, CH_2); 6.41–6.43 (d, 1H, pyrimidone-H at sixth position); 6.6–6.69 (d, 1H, pyrimidone-H at fifth position); 7.25–7.41 (d, 2H, Ar-H); 7.43–7.59 (s, 1H, pyrimidone-H at second position); 7.71–7.82 (d, 2H, Ar-H); 10.6 (bs, 2H, NH); MS (EI): *m/z* (75%) M^+ 356; Anal. calcd. for $C_{14}H_{11}F_3N_4O_4$ (356): C, 47.20; H, 3.11; F, 16.00; N, 15.73. Found: C, 47.30; H, 3.25; F, 16.10; N, 15.62%.

5i: Yield: 51%; mp: 265–267°C; IR (KBr): 1605 (C=O); 1625 (amide, C=O); 3690–3505 cm^{-1} (NH–NH); ^1H NMR (DMSO-d_6) δ: 4.75 (s, 2H, CH_2); 6.42–6.44 (d, 1H, pyrimidone-H at sixth position); 6.71–6.79 (d, 1H, pyrimidone-H at fifth position); 7.3–7.45 (d, 2H, Ar-H); 7.51–7.6 (s, 1H, pyrimidone-H at second position); 7.8–7.89 (d, 2H, Ar-H); 10.8 (bs, 2H, NH); MS (EI): *m/z* (75%) M^+ 317; Anal. calcd. for $C_{13}H_{11}N_5O_5$ (317): C, 49.22; H, 3.49; N, 22.07. Found: C, 49.35; H, 3.62; N, 22.17%.

5j: Yield: 48%; mp: 216.8–218.5°C; IR (KBr): 1615 (C=O); 1665 cm^{-1} (amide, C=O); 3715–3500 cm^{-1} (NH–NH); ^1H NMR (DMSO-d_6) δ: 2.9 (s, 6H, $2CH_3$); 4.73 (s, 2H, CH_2); 6.39–6.48 (d, 1H, pyrimidone-H at sixth position); 6.7–6.77 (d, 1H, pyrimidone-H at fifth position); 7.28–7.4 (d, 2H, Ar-H); 7.45–7.55 (s, 1H, pyrimidone-H at second position); 7.82–7.89 (d, 2H, Ar-H); 11.55 (bs, 2H, NH); MS (EI): *m/z* (72%) M^+ 315; Anal. calcd. for $C_{15}H_{17}N_5O_3$ (315): C, 57.13; H, 5.43; N, 22.21. Found: C, 57.03; H, 5.55; N, 22.12%.

Biology

Xanthine oxidase inhibition studies

The XO inhibitory activity was monitored spectrophotometrically following the absorbance of uric acid at 292 nm under aerobic conditions [25, 26]. Briefly, rat liver was homogenized in 0.01 M Tris–HCl pH (8.0) containing 1 mM EDTA. The homogenate was centrifuged and the supernatant was used as a source of enzyme. It was stored at −80°C until use and the protein content was determined by Lowry's method [29], using bovine serum albumin (BSA) as standard.

XO activity was recorded using a Shimadzu spectrophotometer (UV-1800, Japan). The enzyme assay mixture consisted of 20 mM potassium phosphate buffer (pH 7.4) containing 0.3 mM EDTA and the enzyme source in a total volume of 2 mL. In dose-dependent inhibition studies, the reaction was initiated by the addition of xanthine (50 μM) as the substrate to the above assay mixture and the test compounds. The absorption rate at a wavelength of 292 nm indicates the formation of uric acid at 10 min intervals at ambient temperature. Duplicate assays were repeated thrice. Allopurinol was used as positive control and

DMSO was used as blank. The inhibitory activity of each test compound against XO was indicated by their percentage inhibition values. The percentage inhibition of XO activity was calculated using the following formula:

$$\text{Xanthine oxidase Inhibition}\,(\%) = \frac{\text{Abs control} - \text{Abs sample}}{\text{Abs control}} \times 100$$

Abs control, absorbance of the control reaction (containing all reagents except the test compound); Abs sample, absorbance of the test compound.

Antioxidant activity

DPPH radical scavenging assay

DPPH radical scavenging assay was done according to Yen and Duh [30]. Briefly, 1 mL of DPPH solution (0.1 mM, in 95% ethanol v/v was incubated with different concentrations of the compounds. The reaction mixture was shaken and incubated for 20 min at room temperature, and the absorbance was read at 517 nm against a blank. The antioxidant BHA was used as a positive control in all the assays. The radical scavenging activity was measured as decreased absorbance of DPPH and calculated using the following equation:

$$\text{Scavenging effect}\,(\%) = \left[\frac{A_{\text{control}} - A_{\text{sample}}}{A_{\text{control}}}\right] \times 100$$

Lipid peroxidation assay

LPO inhibitory activity was measured according to Kulkarni et al. [31]. Egg lecithin (3 mg/mL in phosphate buffer, pH 7.4) was sonicated (Hielscher GmbH UP 50H ultra-chill processor sonicator) for 30 min to obtain small membrane liposome vesicles. Different concentrations of the compounds were added to 0.5 mL of liposome mixture. LPO was induced by adding 10 μL of 400 mM $FeCl_3$ and 10 μL of 200 mM L-ascorbic acid. After 60 min of reaction at 37°C, the reaction was stopped by the addition of 1 mL of 0.25 N HCl containing 15% TCA and 0.375% TBA and incubation in a boiling water bath for 15 min. After centrifugation at 10,000 rpm, absorbance of the supernatant was measured at 532 nm. The scavenging effect was calculated using the equation as described for DPPH.

Reducing power assay

The reducing power was measured by incubating the reaction mixture (1 mL) containing the samples in the phosphate buffer (0.2 M, pH 6.6) with potassium ferricynaide (1 g/100 mL water) at 50°C for 20 min. The reaction was terminated by adding TCA (10 g/100 mL water), the mixture was centrifuged at 3000 rpm for 10 min, and the supernatant was mixed with ferric chloride (0.1 g/100 mL of water); the absorbance was measured at 700 nm [32]. Increased absorbance of the reaction mixture indicated increased reducing power.

Hydroxyl radical scavenging activity

The reaction mixture, containing compounds **7a–j** (at different concentrations), was incubated with deoxyribose (15 mM), H_2O_2 (10 mM), $FeCl_3$ (500 μM), EDTA (1 mM), and ascorbic acid (1 mM) in potassium phosphate buffer (100 mM) pH 7.4 for 60 min at 37°C. The reaction was terminated by adding 1 mL TBA (1% w/v) and then heating tubes in a boiling water bath for 15 min. The contents were cooled, and the absorbance of the mixture was measured at 535 nm against the reagent blank [33].

Metal ion chelating assay

The Fe_2^+-chelating ability of the extract was measured by the ferrous iron–ferrozine complex at 562 nm [34]. The reaction mixture containing $FeCl_2$ (2 mM/L) and ferrozine (5 mM/L) along with extracts was adjusted to a total volume of 0.8 mL with methanol, mixed, and incubated for 10 min at room temperature. The absorbance of the mixture was read at 562 nm against a blank. EDTA was used as positive control. The ability of the extract to chelate ferrous ion was calculated using the equation described for DPPH.

Statistical analysis

All experiments were carried out in triplicates and repeated in three independent sets of experiments. Data are shown as means ± SD. The SPSS10.0.5 version for windows (SPSS Software, Inc., USA) computer program was used for statistical analysis. The significance of the study was assessed by one-way ANOVA, followed by post-hoc comparison test. Correlations between quantitative properties were evaluated by calculating the Duncan and Dennett's coefficient. Statistical significance value was set at $p < 0.05$.

Molecular docking

The human milk XO (EC: 1.17.3.2) with PDB entry code: 2CKJ was built using CPH Models server 3.0. The ligands were docked into the active site using the molecular docking software Molegro Molecular Viewer 2008, version 1.2.0 (http://molegro.com) [35] with default parameters for calculating the docking modes of small molecules into protein-binding sites based on their shape complementarity. In this, we have used ChemScore, a scoring function that is derived from regression against receptor–ligand binding free energies [36].

One of the authors (S.A.K.) gratefully acknowledges the financial support provided by Vision Group on Science and Technology, Department of Information Technology, Biotechnology and Science & Technology, Government of Karnataka, Bangalore, under the scheme CISEE-programme.

The authors have declared no conflict of interest.

References

[1] R. Hille, *Chem. Rev.* **1996**, *96*, 2757–2816.

[2] P. Richette, R. Garay, *Expert Opin. Drug Discov.* **2013**, *8*, 183–189.

[3] D. E. Koshland, Jr., *Ann. N Y Acad. Sci.* **1963**, *103*, 630–642.

[4] M. Dixon, E. C. Webb, C. J. R. Thorne, K. F. Tipton, *Enzymes* (3rd edition), Longman, London **1979**, p. 126.

[5] R. W. Rundes, J. B. Wyngaarden, *Ann. Rev. Pharmacol.* **1969**, *9*, 345–362.

[6] M. D. Harris, L. B. Siegel, J. A. Alloway, *Am. Fam. Physician* **1999**, *59*, 925–934.

[7] J. H. Klippel, *Primer on the Rheumatic Diseases* (13th edition), Springer, New York, USA **2008**.

[8] F. Perez-Ruiz, M. Calabozo, G. G. Erauskin, *Arthritis Rheum.* **2002**, *47*, 610–613.

[9] M. Senevirathne, S. Kim, N. Siriwardhana, J. Ha, K. Lee, Y. Jeon, *Food Sci. Tech. Int.* **2006**, *12*, 27–28.

[10] K. Ichida, Y. Amaya, K. Okamoto, T. Nishino, *Int. J. Mol. Sci.* **2012**, *13*, 15475–15495.

[11] J. S. Beckman, W. H. Koppenol, *Am. J. Physiol.* **1996**, *271*, 1424–1437.

[12] J. F. Turrens, *J. Physiol.* **2003**, *552*, 335–344.

[13] J. de Leiris, A. Rakotovao, F. Boucher, *Heart Metab.* **2006**, *31*, 5–7.

[14] E. Abele, R. Abele, O. Dzenitis, E. Lukevics, *Chem. Heterocycl. Comp.* **2003**, *39*, 8–10.

[15] Y. M. A. Hiari, A. M. Quisi, M. M. Abadelah, W. Voelter, *Monat. Chem.* **2006**, *137*, 243–249.

[16] B. C. Hong, Y. Jiang, Y. Chang, S. J. Lee, *Chinese Chem. Soc.* **2006**, *53*, 647–652.

[17] M. K. Manal, W. M. Lamia, K. Mohammed, H. abd el, T. Ahmed Negmeldin, *Sci. Pharm.* **2012**, *80*, 531–545.

[18] T. D. Venu, S. A. Khanum, F. Aiysha, B. K. Manuprasad, S. Shashikanth, R. Mohamed, B. S. Vishwanath, *Bioorganic Med. Chem. Lett.* **2008**, *18*, 4409–4412.

[19] A. Rykowski, W. Pucko, *Acta Pol. Pharm.* **1997**, *54*, 325–329.

[20] M. S. Manhas, S. D. Sharma, S. G. Amine, *J. Med. Chem.* **1979**, *15*, 106–112.

[21] I. A. Kharizomenova, A. N. Grinev, N. V. Samsonva, E. K. Panisheva, N. V. kaplina, I. S. Nikolaeva, T. V. Pushkina, G. N. Pershin, *Khim Farm Zh.* **1981**, *15*, 40–44.

[22] A. E. Rashad, M. A. Ali, *Nucleos. Nucleot. Nucl.* **2006**, *25*, 17–28.

[23] A. Padmaja, T. Payani, G. D. Reddy, V. Padmavathi, *Eur. J. Med. Chem.* **2009**, *44*, 4557–4566.

[24] K. R. Sathisha, S. A. Khanum, J. N. S. Chandra, F. Ayisha, S. Balaji, K. Marathe, G. Shubha, K. S. Rangappa, *Bioorg. Med. Chem.* **2011**, *19*, 211–220.

[25] R. S. Kadam, K. R. Iyer, *Indian J. Pharm. Sci.* **2007**, *69*, 41–45.

[26] G. Litwack, J. W. Bothwell, J. N. Williams, R. J. Elvehjem, *J. Biol. Chem.* **1952**, *200*, 303–310.

[27] S. Gupta, L. M. Rodrigues, A. P. Esteves, A. M. F. Oliveira-Campos, M. S. J. Nascimento, N. Nazareth, H. Cidade, M. P. Neves, E. Fernandes, M. Pinto, N. M. F. S. A. Cerqueira, N. Bras, *Eur. J. Med. Chem.* **2008**, *43*, 771–780.

[28] A. Julie, J. A. Ross, C. M. Kasum, *Annu. Rev. Nutr.* **2002**, *22*, 19–34.

[29] O. H. Lowry, N. J. Rosebrough, A. L. Farr, R. J. Randall, *J. Biol. Chem.* **1951**, *193*, 265–275.

[30] G. C. Yen, P. D. Duh, *J. Agri. Food Chem.* **1994**, *42*, 629–632.

[31] A. P. Kulkarni, S. M. Aradhya, S. Divakar, *Food Chem.* **2004**, *87*, 551–557.

[32] G. C. Yen, H. Y. Chen, *J. Agric. Food Chem.* **1995**, *43*, 27–32.

[33] B. Halliwell, J. M. C. Gutteridge, O. I. Aruoma, *Anal. Biochem.* **1987**, *165*, 215–219.

[34] E. A. Decker, B. Welch, *J. Agric. Food Chem.* **1990**, *38*, 674–677.

[35] A. W. Schuttelkopf, D. M. F. V. Aalten, *Acta Crystallogr.* **2004**, *68*, 1355–1363.

[36] R. Thomsen, M. H. Christensen, *J. Med. Chem.* **2006**, *49*, 3315–3321.

